CIVIL AND ENVIRONMENTAL ENGINEERING REPORTS

No. 1 2005

TRI-AXIAL TESTS FOR BRITTLE MATERIALS: MOTIVATION, TECHNIQUE, RESULTS

Andrzej LITEWKA[1], Leszek SZOJDA[2]
[1] Universidade da Beira Interior, Departamento de Engenharia Civil, Covilhã, Portugal
[2] Silesian University of Technology, Department of Civil Engineering, Gliwice, Poland

The aim of the paper is to explain the experimental technique used in tri-axial material tests and to supply new and more general experimental data on deformability and fracture of ceramics and cementitious composites. Such experimental data are necessary to formulate theoretical models capable to describe the mechanical behaviour of brittle rock-like materials. The program of experiments consisted of two different tests performed under tri-axial loading and also of uni-axial compression that supplied preliminary data necessary to calibrate the material. The second objective of this study is to present the potentialities of own phenomenological model based on continuum damage mechanics and on theory of tensor function representation that can be used to describe the response of brittle rock-like material subjected to tri-axial state of stress.

Keywords: experimental methods, tri-axial tests, rock-like brittle materials, stresses at fracture

1. INTRODUCTION

The progress in mechanics of solids and structures requires mutually interrelated extensive theoretical and experimental studies of mechanical properties of structural materials. Such a necessity particularly exists when new materials are used and when advanced theoretical models are formulated to describe the physical processes observed in solids subjected to multi-axial state of stress. Requirements of modern technology gave rise to deeper experimental studies of mechanical properties of metals subjected to complex loading at elevated temperature that prevails in engines of space rockets, aircrafts and automobiles and also in steam turbines of conventional and nuclear power stations. That is why

ISBN 83-89712-71-7

extensive experimental tests were performed for metals under uni-axial and bi-axial loading to study such physical phenomena like large plastic deformations, internal damage growth and creep rupture of metals that decide on safety of structural elements. Relatively small amount of respective experimental data on creep rupture problems of metals subjected to tri-axial state of stress is available in the literature [3, 11, 16, 17, 28].

Brittle rock-like materials could be considered as a second group of structural materials where some attempts of tri-axial experimental tests were reported. Strong motivation for such experiments exists in rock and soil mechanics where superposition of axial compression and lateral confining pressure constitutes the standard state of stress in these materials in natural deposits. Some rather incomplete experimental data on mechanical behaviour of rocks subjected to that specific case of tri-axial state of stress can be found in monographs on rock mechanics [9, 10, 13, 34]. These data and similar but very limited results available for concrete [8, 14, 33, 39] give some preliminary information on behaviour of brittle rock-like material tested under multi-axial state of stress. Wide utilisation ceramics and cementitious composites requires deeper studies of such phenomena like load or deformation induced anisotropy that develops in loading process due to internal oriented damage growth. This problem was studied experimentally by Mitrofanov and Dovzenko [30], Bogucka et al. [6], Litewka et al. [25] and theoretically by Karpenko [18] and Baikov [1]. Simultaneously, new approach based on the methods of continuum damage mechanics was used to formulate some phenomenological models capable to describe the mechanical behaviour of brittle rock-like materials in presence of oriented damage growth [2, 15, 19, 24, 26, 27, 32]. All those theoretical descriptions are based on limited experimental data, particularly for tri-axial state of stress and were verified for some specific cases of loading only. To obtain more realistic theoretical description of overall material response that could account for oriented damage growth and development of damage induced anisotropy the further extensive experimental studies are needed.

The aim of this note is to supply new and more general experimental data on mechanical response of brittle materials subjected to tri-axial state of stress and to explain the experimental technique used. To obtain more complete information on deformability, damage growth and fracture of these materials two different tri-axial tests were used. The program of loading consisted of these two cases of tri-axial loading and also of uni-axial compression that supplied preliminary data necessary to calibrate the material. The first case of tri-axial loading was a superposition of hydrostatic pressure and axial compression and the second case consisted in simultaneous action of hydrostatic pressure and bi-axial uniform compression. The tests in both cases of tri-axial compression were performed for several levels of the hydrostatic pressure. Preliminary results of

these experiments and their practical applications are shown in [29, 35, 36, 37]. The second objective of the study presented here is to show the potentialities of own phenomenological model [24, 27] based on continuum damage mechanics [23, 31] and on theory of tensor function representation [4, 5] that can be used to describe the response of brittle rock-like material subjected to tri-axial state of stress.

2. SPECIMENS AND LOADING

Available experimental data on mechanical behaviour of brittle rock-like materials obtained by Kupfer [20], Ehm and Schneider [12], Thienel et al. [38] and Ligęza [22] concern to concrete subjected to plane state of stress. Those experiments performed on suitably shaped concrete plates required special technique of bi-axial loading and appropriate test procedure described by Kupfer and Zegler [21]. Much more technical problems are faced when testing brittle rock-like materials under tri-axial state of stress and that is why rather limited amount of the respective experimental data on the mechanical behaviour of materials subjected to such a state of stress is available in the literature. This applies not only to brittle rock-like solids but also to other structural materials. Very strong motivation to perform the tri-axial tests exists in the case of metals where creep rupture problems at elevated temperature decide on life-time of structural elements subjected to multi-axial state of stress. To this end specially designed cylindrical notched bars proposed by Bridgeman [3] were used to obtain relatively uniform tri-axial state of stress localized at the bottom of the notch. Further development and practical applications of this experimental procedure can be found in [11, 17, 28]. Improved experimental technique that can be used to produce well defined uniform tri-axial state of stress was proposed by Hayhurst and Felce [16]. They designed three dimensional cruciform metal specimen subjected to tri-axial loading to obtain arbitrary combination of three principal stresses in central cube of the specimen.

Unfortunately, those well known experimental techniques elaborated for tri-axial loading of metals cannot be used in the case of brittle rock-like materials and that is why very limited amount of respective experimental data can be found in the literature for such solids. Available experimental results concern mainly to rocks subjected to simultaneous action of axial compressive load represented by compressive stress σ_V and hydrostatic pressure p, referred to as a confining pressure. This specific case of tri-axial loading shown in Fig. 1a corresponds to the state of stress observed in rocks and soils in natural deposits and that is why was frequently used to study the properties of such materials. Some rather incomplete data that are oriented for requirements of rock mechanics can

be found in monographs by Cristescu and Hunsche [9], Derski et al. [10] and Goodman [13]. These data and very scarce similar results available for concrete

Table 1. Experimental data and constants used in analysis of tri-axial state of stress of mortar and brick

Constant	Unit	Mortar	Brick
E_0	MPa	8030	2420
ν_0	-	0.175	0.105
f_c	MPa	-7.39	-11.49
A	MPa^{-2}	2500×10^{-5}	1064×10^{-5}
B	MPa^{-2}	100.0×10^{-5}	100.0×10^{-5}
C	MPa^{-1}	-1.000×10^{-5}	-1.500×10^{-5}
D	MPa^{-1}	2.188×10^{-5}	3.508×10^{-5}
F	-	0.9400	0.6300

reported by Chen [8] and Neville [33] give some information on behaviour of brittle rock-like material and make it possible to conclude that confining pressure increases the axial load that can be sustained. Moreover, in the limit case when hydrostatic pressure only is applied, practically linear mechanical response of a material described by the law of elastic change of volume is observed (Carvalho et al. [7]).

To obtain more complete information on plastic deformation, oriented damage growth and fracture for ceramics, concrete, cementitious composites and rocks further experimental studies are needed. That is why the classical procedure of tri-axial loading seen in Fig. 1a was extended by one more tri-axial test explained in Fig. 1b. The experimental results presented here were obtained for specimens of mortar and brick shown in Fig. 2. The height and diameter of the cylindrical specimens used were equal to 12 cm and 6 cm, respectively. The tests were performed in testing machine ZD40 of 400 kN capacity combined with the hydraulic attachment shown in Fig. 2 necessary to apply a lateral

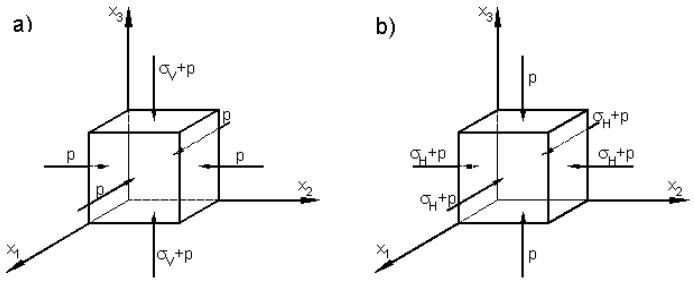

Fig. 1. Configuration of the stress tensor components for two cases of tri-axial state of stress: a) State I, b) State II

compression to the specimens tested. The program of loading consisted of uni-axial compression and two cases of tri-axial loading referred to as State I and State II and shown in Figure 1. The objective of the test performed under uni-axial compression was to determine the initial Young modulus E_0 and Poisson ratio v_0 as well as to measure the uni-axial compressive strength f_c for both materials tested. The numerical values of the above mentioned constants together with the other material parameters included in the theoretical model adopted in this paper are shown in Table 1.

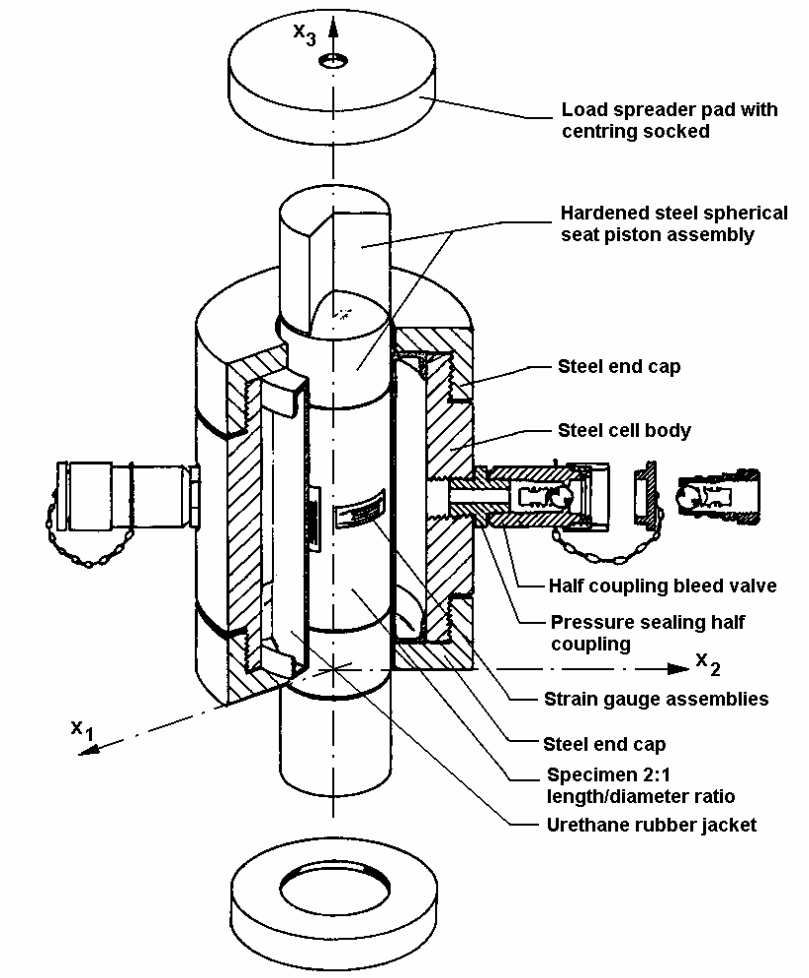

Fig. 2. Apparatus for tri-axial compression tests and specimen tested

The objective of the tests under tri-axial state of stress was to determine the respective stress-strain curves and to measure the stresses at material fracture for prescribed loading program. Various combinations of the stress tensor components and at least two different loading paths are necessary to supply information on the shape of the limit surface at material failure subjected to tri-axial states of stress. The loading paths for State I and State II of tri-axial compression shown in Figure 3 consisted of two stages. The Stage 1 was the same in both cases of tri-axial loading and consisted in a monotonic increase of hydrostatic pressure up to prescribed value p. In the Stage 2 of the first tri-axial state of stress (State I) the vertical normal stress σ_V was increased up to material failure that occurs for $\sigma_{3f} = p + \sigma_V$. The second tri-axial state of stress (State II) is a combination of hydrostatic pressure p and uniform bi-axial compression. In the Stage 2 of this case of loading two horizontal components σ_H of uniform bi-axial state of stress were increased simultaneously up to material failure that corresponds to $\sigma_{1f} = \sigma_{2f} = p + \sigma_H$. Such a programme of loading required certain

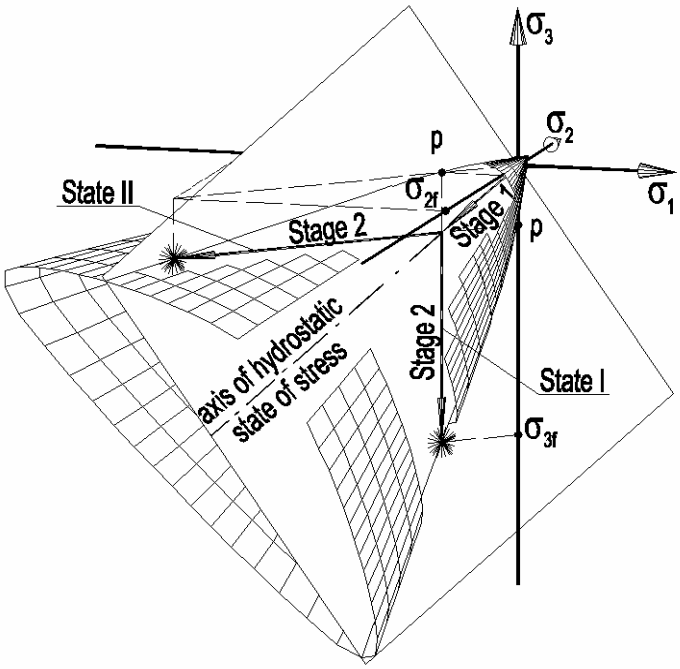

Fig. 3. Limit surface at material fracture and loading paths: * point corresponding to material fracture

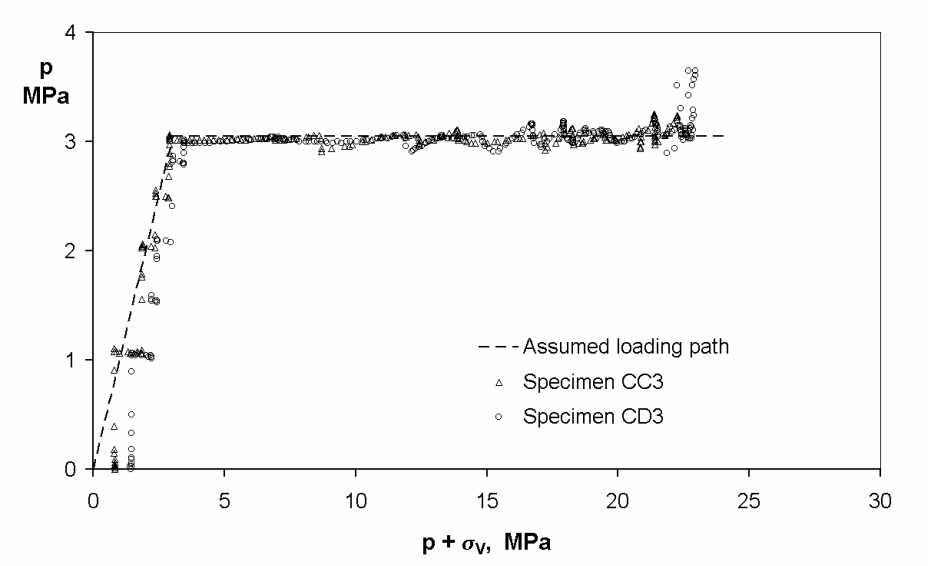

Fig. 4. Variation of the stress tensor components along the loading path for State I of tri-axial compression for specimens of brick (p = -3.05 MPa)

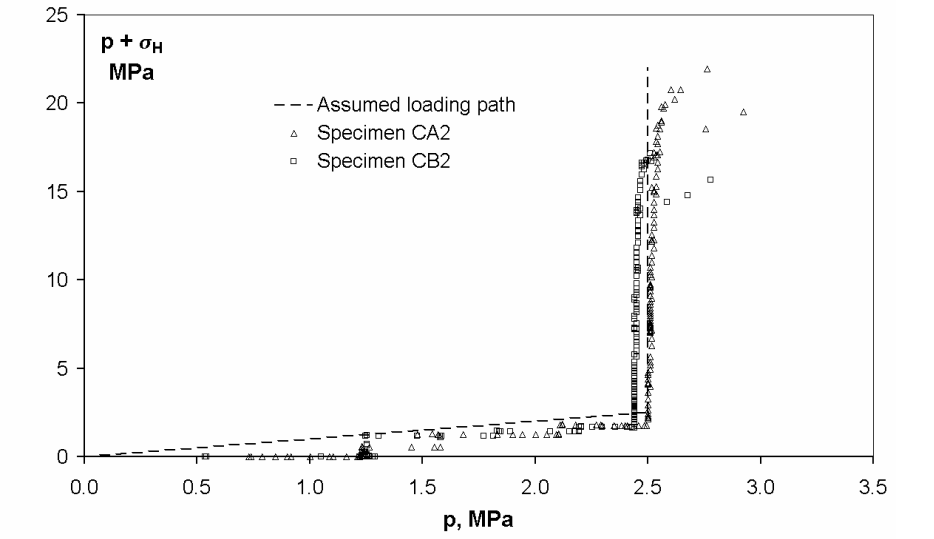

Fig. 5. Variation of the stress tensor components along the loading path for State II of tri-axial compression for specimens of brick (p = -2.50 MPa)

accuracy of the hydraulic system of the testing machine. Practically it is impossible to obtain perfectly rectilinear form of each part of the loading path and some oscillations of the stress tensor components occur as shown in Fig. 4 and 5. It is seen that such variations of real values of the stresses are larger at the end of each loading path. This effect is due to relatively large deformations of the specimens before material fracture.

3. STRAIN MEASUREMENT

Deformation of the specimen subjected to tri-axial loading should be measured at each stage of the loading process to supply information necessary to construct the stress-strain relations for material tested. Because of limited space within the hydraulic cylinder used to apply lateral compression to the specimen very small extensometers can be employed. That is why four electrical resistance strain gauges arranged in the form of two rosettes glued on the opposite sides of the specimen were used to measure longitudinal and lateral deformations of the specimen. Configuration of one of the rosettes and the specimen tested are seen in Fig. 2. Unfortunately, these strain gauges were subjected to direct action of hydrostatic pressure applied to the lateral surface of the specimen. It means that the dimensions of the electric conductor of each strain gauge were changed not only by the deformation of the specimens but also by hydrostatic pressure. Such a pressure applied directly to the strain gauge reduced the lateral dimension of the conductor and increased its length. In this situation the variation of the resistance of the conductor was increased and corresponding readings of strains contained certain unknown systematic error. This unknown contribution of the hydrostatic pressure reduced the readings for negative strains and increased the readings for positive strains of the specimens. Such effect could be eliminated by means of special compensating strain gauge subjected to the same hydrostatic pressure and glued on the surface of sufficiently rigid element that has no deformation due to load applied. Configuration of the hydraulic cylinder shown in Fig. 2 and its dimensions preclude any possibility to use the direct method of compensation of the hydrostatic pressure effect. More practical seems to be indirect compensation that was used in experiments presented in this paper. To this end the experimental results obtained for strains in Stage 1 of each loading path were compared with the theoretical predictions. In this initial stage of loading the specimens were subjected to the hydrostatic state of stress

$$\sigma_{ij} = \delta_{ij} p \ , \tag{3.1}$$

where σ_{ij} is the stress tensor, δ_{ij} is the Kronecker delta and p is the value of applied hydrostatic pressure. It was shown experimentally (Carvalho et al. [7]) that

the state of stress expressed by Eq. (3.1) does not produce any damage of the material what results in perfectly linear stress strain relation described by the law of variation of volume of linear elastic material

$$\sigma_m = \frac{E_0}{3(1-2\nu_0)}\varepsilon_{kk} \ , \tag{3.2}$$

where $\sigma_m = p$ is the mean normal stress and $\varepsilon_{kk} = 3\varepsilon$ is the sum of the diagonal components ε of the respective strain tensor. The numerical values of the initial Young modulus E_0 and initial Poisson coefficient ν_0 can be found in Table 1.

Comparison of the straight line represented by Eq. (3.2) with the initial readings made for the respective strain gauges is shown for mortar and for brick in Fig. 6. It is seen from this figures that significant deviation of experimental points from theoretical prediction occurs for both materials tested. Moreover it is seen that the difference between the strains determined by theoretical straight line and those indicated by respective line that approximates the distribution of

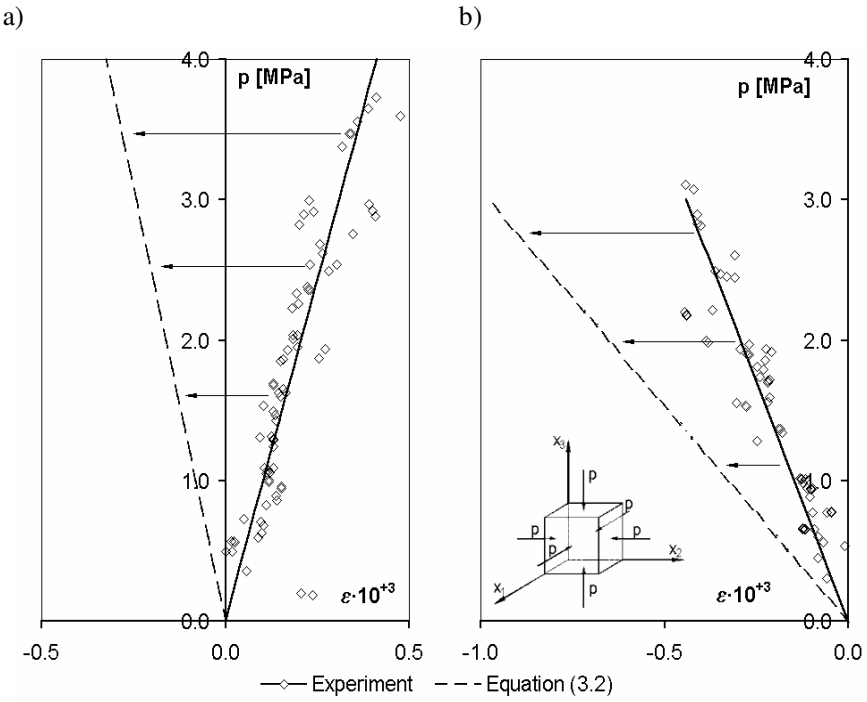

Fig. 6. Experimental readings of strains made for strain gauges subjected to direct action of hydrostatic pressure and theoretical prediction for: a) specimens of mortar, b) specimens of brick

experimental points is practically the same for mortar and brick. This difference defines the influence of hydrostatic pressure for readings made for the strain gauges used to measure the deformation of the specimens. It was found from Fig. 6 that the coefficient compensating the effect of hydrostatic pressure is equal to

$$\varepsilon_{\text{comp}}^{b} = -0.000180\ \text{MPa}^{-1} \tag{3.3}$$

for brick and

$$\varepsilon_{\text{comp}}^{m} = -0.000184\ \text{MPa}^{-1} \tag{3.4}$$

for mortar. Both values presented by Eq. (3.3) and (3.4) are practically the same what means that effect of hydrostatic pressure for readings made for the strain gauges does not depend on the properties of the strata material on which the strain gauges are glued. On the other hand, one could presume that the coefficient of the correction should depend on the material of the electric conductor and on the type of the strain gauges used.

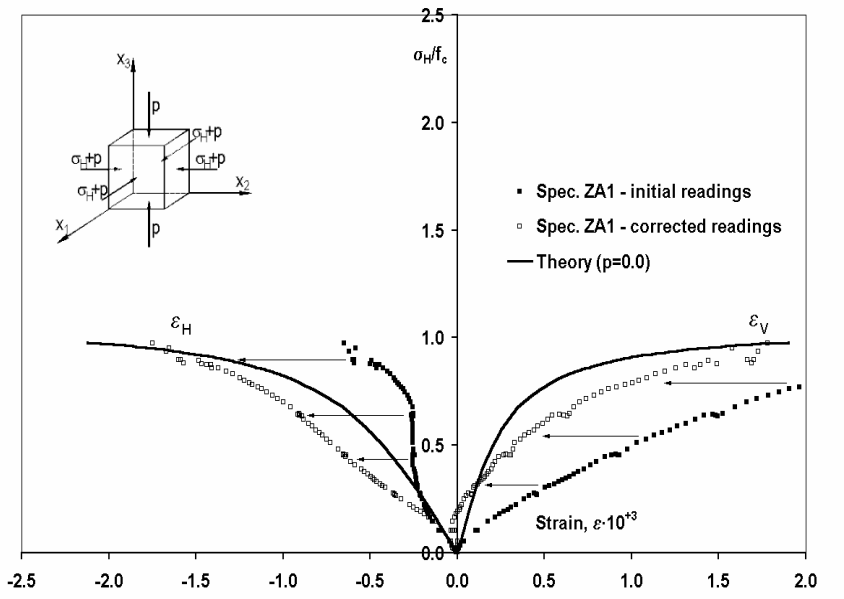

Fig. 7. Correction of experimental stress-strain curves for bi-axial uniform compression (State II for p = 0) for mortar to compensate the effect of direct action of hydrostatic pressure applied to strain gauges and theoretical predictions

Practical application of this method of compensation of the effect of hydrostatic pressure applied directly to the strain gauges is shown in Fig. 7 and 8 for two cases of the State II of multi-axial compression of the specimens made of brick and mortar. To obtain the experimental stress-strain curves, the initial readings made for the strain gauges were corrected taking into account the values of the respective coefficients of compensation defined by Eq. (3.3) and (3.4). In this specific form of tri-axial loading seen in Fig. 1b the total value of the lateral pressure applied directly to the strain gauges equal to $p_{\text{Total}} = p + \sigma_H$ increases monotonically in Stage 2 of loading path up to material failure. It should be noted that in State I of tri-axial compression shown in Fig. 1a such a compensation of experimentally determined stress-strain curves is not necessary. The Stage 2 of the loading path for State I consists in monotonic increase of vertical stress σ_V only whereas the pressure p applied to the lateral surface of the specimen is constant.

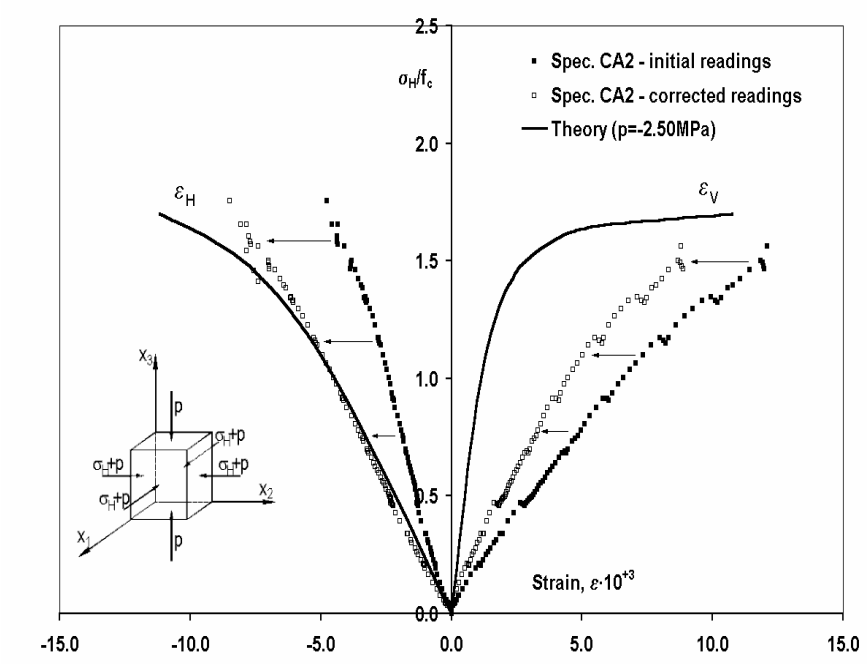

Fig. 8. Correction of experimental stress-strain curves for tri-axial compression (State II for p = -2.50 MPa) for brick to compensate the effect of direct action of hydrostatic pressure applied to strain gauges and theoretical predictions

The stress-strain curves seen in Fig. 7 and 8 present the relation between variable components of bi-axial uniform compression σ_H and horizontal or vertical strains determined from the relations

$$\varepsilon_H = \varepsilon_1 - \frac{1-2\nu_0}{E_0} p \tag{3.5}$$

$$\varepsilon_V = \varepsilon_3 - \frac{1-2\nu_0}{E_0} p\,, \tag{3.6}$$

where $\varepsilon_1 = \varepsilon_2$ and ε_3 are the principal strains measured experimentally for the specimens tested.

4. DISCUSSION OF THE RESULTS

Experimental results presented in this paper for brick and mortar tested under tri-axial compression were compared with the theoretical predictions obtained from own phenomenological model. This theoretical description is based on the methods of the damage mechanics and on assumption of tensorial nature of the material damage. That is why the symmetric second rank damage tensor was used as a variable responsible for deterioration of the material internal structure. Explicit form of the relevant constitutive equations was found by employing the methods of the theory of tensor function representations as applied in solid mechanics [4, 5]. Some results of possible application of this mathematical approach to describe a non-linear behaviour of a concrete and rocks, including the experimental verification, were presented in [24, 25, 26, 27]. However, the new experimental data on tri-axial state of stress shown in this note required some modifications and generalizations of the constitutive equations presented in [26, 27]. Improved mathematical model used here consists of the stress strain relations for anisotropic elastic solids expressed in the form of the following tensor function

$$\begin{aligned}\varepsilon_{ij} = &-\frac{\nu_0}{E_0}\delta_{ij}\sigma_{kk} + \frac{1+\nu_0}{E_0}\sigma_{ij} + \\ &+ C(\delta_{ij}D_{kl}\sigma_{kl} + D_{ij}\sigma_{kk}) + 2D(\sigma_{ik}D_{kj} + D_{ik}\sigma_{kj})\end{aligned} \tag{4.1}$$

that describes the anisotropic elastic non-linear response of the damaged material. Equation (4.1) contains the strain tensor ε_{ij}, two constants C and D to be determined experimentally and the second order symmetric damage effect tensor D_{ij} responsible for the current state of internal structure of the material defined in [23].

Analysis of the experimental results presented in [24, 25, 26, 27] shows that the deterioration of the material structure starts at the beginning of the loading process and that an amount and configuration of the damage depends on the state of stress applied. That is why it was assumed that the damage is a function of the load applied to the material represented by the stress tensor components. In this situation the damage evolution equation could be formulated in the form of the following tensor function representation

$$\Omega_{ij} = As_{kl}s_{kl}\left(1+\frac{227\det\sigma_{pq}}{200\left|\det\sigma_{rs}\right|+\left|\sigma_{ll}^{3}\right|}\right)^{F}\delta_{ij}+ \\ +B\sqrt{\sigma_{kl}\sigma_{kl}}\left(1+\frac{227\det\sigma_{pq}}{200\left|\det\sigma_{rs}\right|+\left|\sigma_{ll}\right|}\right)^{F}\sigma_{ij} \tag{4.2}$$

where Ω_{ij} is a classical second order damage tensor. Equation (4.2) contains the stress deviator s_{kl} and three unknown material parameters A, B, F to be determined experimentally. The first term of the Eq. (4.2) represents the isotropic damage and the second one accounts for the oriented damage due to different effects of the stress tensor components. Five constants *A, B, C, D* and *F* seen in Eq. (4.1) and (4.2) can be determined experimentally by using various methods discussed in [6, 24, 27]. The numerical values of these constants for brick and mortar were obtained by employing the specific method explained in [27]. The respective data for *A, B, C, D* and *F* used in further discussion are shown in Table 1.

As was shown earlier [23] the damage tensor Ω_{ij}, is not sufficient to describe the strength and stiffness reduction of the damaged material, and that is why it was necessary to define another state variable called the damage effect tensor D_{ij}. The relation

$$D_i = \frac{\Omega_i}{1-\Omega_i}\ , \quad i=1,\ 2,\ 3 \tag{4.3}$$

between the principal values Ω_1, Ω_2 and Ω_3 of the damage tensor Ω_{ij} and the principal components D_1, D_2 and D_3 of the damage effect tensor D_{ij} was formulated in [23]. The principal components of the damage effect tensor calculated from Eq. (4.3) are ranging from zero for an undamaged material to infinity for a fully damaged material. It means that increasing damage expressed in terms of the damage effect tensor gradually reduces the stiffness and strength of the material to zero.

Experimental results presented in this paper concern to two specific cases of the tri-axial loading referred to as State I and State II. To compare these re-

sults with theoretical predictions it is necessary to express Eq. (4.1) and (4.2) in terms of the stress tensor

$$\sigma_{ij} = \begin{bmatrix} \sigma_{11} = p & 0 & 0 \\ 0 & \sigma_{22} = p & 0 \\ 0 & 0 & \sigma_{33} = \sigma_V + p \end{bmatrix} \tag{4.4}$$

for State I and

$$\sigma_{ij} = \begin{bmatrix} \sigma_{11} = \sigma_H + p & 0 & 0 \\ 0 & \sigma_{22} = \sigma_H + p & 0 \\ 0 & 0 & \sigma_{33} = p \end{bmatrix} \tag{4.5}$$

for State II. This made it possible to construct the theoretical stress-strain curves for various combinations of the stress tensor components. The comparison of such theoretical curves with corresponding experimental results is presented in Fig. 7, 8, 9 and 10. The theoretical values of the principal strains $\varepsilon_1 = \varepsilon_2$ and ε_3 where determined from Eq. (4.1) and (4.2) taking into account Eq. (4.3). The

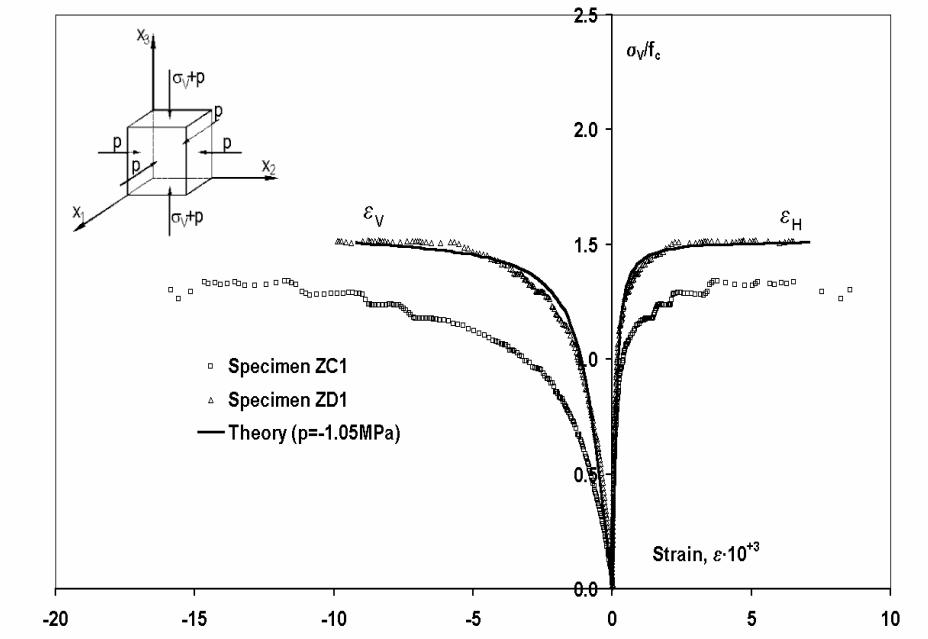

Fig. 9. Experimental and theoretical stress-strain curves for tri-axial compression (State I for p = -1.05 MPa) for mortar

Table 2. Experimental and theoretical stress at fracture for brick and mortar subjected to State I of tri-axial state of stress

Specimen	Material	Hydrostatic pressure MPa	Failure stress σ_{3f} MPa		Difference %
			Experiment	Theory	
ZC1	Mortar	-1.05	-10.90	-12.26	-11.1
ZD1	Mortar	-1.05	-12.20	-12.26	-0.5
CC3	Brick	-3.05	-22.25	-21.53	+3.3
CD3	Brick	-3.05	-22.96	-21.53	+6.6

horizontal and vertical strains ε_H and ε_V shown in Fig. 7, 8, 9 and 10 are given by Eq. (3.5) and (3.6). Fairly good agreement seen in these figures corroborates the validity of the theoretical model proposed.

Theoretical model presented in this paper can also be used to determine the maximum stresses that can be sustained by the material subjected to multi-axial state of stress. According to the rules of the damage mechanics the material looses its continuity when at least one of the principal components Ω_1,

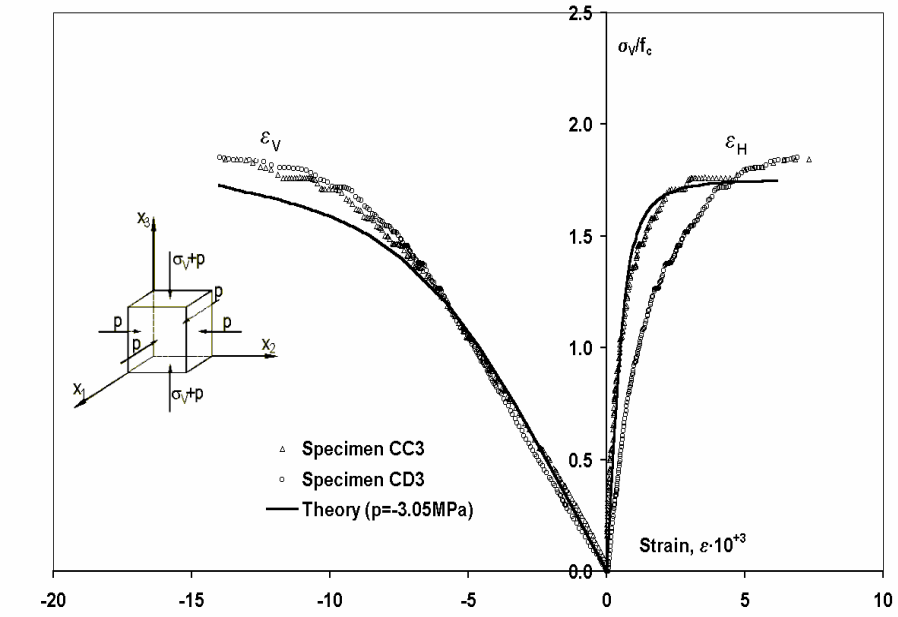

Fig. 10. Experimental and theoretical stress-strain curves for tri-axial compression (State I for p = -3.05 MPa) for brick

Table 3. Experimental and theoretical stress at fracture for brick and mortar subjected to State II of tri-axial state of stress

Specimen	Material	Hydrostatic pressure MPa	Failure stress $\sigma_{1f} = \sigma_{2f}$ MPa		Difference %
			Experiment	Theory	
ZA1	Mortar	0	-7.19	-7.75	-7.2
CA2	Brick	-2.50	-21.94	-22.44	-2.2

Ω_2 or Ω_3 of the damage tensor Ω_{ij} determined from Eq. (4.2) reaches the limit value equal to unity. In such a case the stiffness of the material decreases to zero what corresponds to practically horizontal part of the theoretical stress-strain curves shown in Fig. 7, 8, 9 and 10. Comparison of the stresses at material fracture determined experimentally with theoretical prediction is shown in Tables 2 and 3. The maximum difference between theoretical and experimental results seen in Table 2 for the specimen ZC1 of mortar is equal to 11.1%. The discrepancies obtained for other specimens are much smaller and the average difference determined for six specimens presented here does not exceed 2%. This relatively good agreement shows that overall accuracy of the theoretical model used in this paper is satisfactory.

5. CONCLUSIONS

Classical tri-axial test of confined axial compression used in rock mechanics is not sufficient to study the mechanical behaviour of brittle materials subjected to multi-axial state of stress. To obtain more complete information on material response at least two different tri-axial tests are necessary. That is why one more test was proposed in this paper. Application of this additional test required the special method of compensation of the effect of hydrostatic pressure that was applied directly to electrical resistance strain gauges. The indirect compensation method used here seems to be accurate enough to obtain experimental stress-strain curves.

Theoretical model based on the methods of continuum damage mechanics combined with the theory of tensor function representations used in this paper made it possible to describe experimentally determined mechanical properties of mortar and brick. It was found that theoretical stress-strain curves for tri-axial loading obtained from the relevant equations show satisfactory agreement with experimental data. Fairly good agreement of the experimental data and theoretical predictions was also obtained for the stresses at material fracture. Increasing compressive strength of brittle rock-like materials detected in experiments for

specimens subjected to confined axial compression was also observed in new tri-axial test used here. This phenomenon can be explained theoretically within the mathematical model proposed. Thus, the experimental technique adopted and phenomenological model used in this paper proved to be accurate enough to obtain information necessary to understand the phenomena observed in tri-axial loading of brittle rock-like materials.

Acknowledgements
This work was done within the F.U.T. Program C.E.C. U.B.I. and K.B.N. Grant 5 T07E 02825.

REFERENCES

1. Baikov V.N.: *Particular features of concrete fracture due to its orthotropic deformation*, Beton Zelezobeton, 9 (1990) 19-21, (in Russian).
2. Basista M.: *Micromechanical and lattice modeling of brittle damage*, Warsaw, I.F.T.R. Reports, 3/2001.
3. Bridgman P.W.: *Studies in large plastic flow and fracture*, New York, McGraw Hill 1952.
4. Betten J.: *Anwendungen von Tensorfunktionen in der Kontinuumsmechanik anisotroper Materialen*, Zeitschrift für Angewandte Mathematik und Mechanik, **78**, 8 (1998) 507-521.
5. Boehler J.P.: *Applications of tensor functions in solid mechanics*, Wien, Springer-Verlag 1987.
6. Bogucka J., Dębiński J., Litewka A., Mesquita A.B.: *Experimental verification of mathematical model for oriented damage of concrete*, Mecânica Experimental, 3 (1998) 11-18.
7. Carvalho F.C.S., Chen C.N., Labuz J.F.: *Measurements of effective elastic modulus and microcrack density*, International Journal of Rock Mechanics and Mining Sciences, **34**, 3-4 (1997) paper nr. 043.
8. Chen W.F.: *Plasticity of reinforced concrete*, McGraw-Hill, New York 1982.
9. Cristescu N.D., Hunsche U.: *Time effects in rock mechanics*, John Wiley & Sons, Chichester 1998.
10. Derski W., Izbicki R., Kisiel I., Mróz Z.: *Rock and soil mechanics*, Amsterdam-Warsaw, Elsevier-P.W.N. 1989.
11. Dyson B.F., Loveday M.S.: *Creep fracture in Nimonic 80A under triaxial tensile stressing*, in: Creep in Structures, eds. A.R.S. Ponter, D.R. Hayhurst, Berlin, Springer Verlag 1981, 406-421.

12. Ehm C., Schneider U.: *Biaxial testing of reactor concrete*, in: Transactions of 8th International Conference on Structural Mechanics in Reactor Technology, Vol. H, North Holland, Brusselles 1985, 349-354.
13. Goodman R.E.: *Introduction to rock mechanics*, New York, John Wiley & Sons 1989.
14. Green S.J., Swanson S.R.: *Static constitutive relations for concrete*, AFWL-TR-72-244, U.S. Air Force Weapon Lab., Kirtland A.F. Base, NM. 1973.
15. Halm D., Dragon A.: *An anisotropic model of damage and frictional sliding for brittle materials*, European J. of Mech., A/Solids, **17**, 3 (1998) 439-460.
16. Hayhurst D.R., Felce I.D.: *Creep rupture under tri-axial tension*, Engineering Fracture Mechanics, **25** (1986) 645-664.
17. Hayhurst D.R., Leckie F.A.: *Design of notched bars for creep-rupture testing under tri-axial stress*, Int. J. of Mech. Sciences, **19** (1977) 147-159.
18. Karpenko N.J.: *On formulation of general orthotropic model of concrete deformability*, Stroitielnaja Mekhanica i Rascot Sooruzhenij, 2 (1987) 31-36, (in Russian).
19. Kuna-Ciskał H., Skrzypek J.: *CDM based modeling of damage and fracture mechanisms in concrete under tension and compression*, Engineering Fracture Mechanics, **18**, (2002) 681-698.
20. Kupfer H.: *Das Verhalten des Betons unter mehrachsiger Kurzzeitbelastung unter besonderer Berucksichtigung der zweiachsiger Beanspruchung*, Deutcher Ausschluss fur Stahlbeton, 229 (1973) 1-105.
21. Kupfer H., Zegler C.: *Bau un Erprobung einer Versuchseinrichtung fur zweiachsige Belastung*, Deutcher Ausschluss fur Stahlbeton, 229 (1973) 107-131
22. Ligęza W.: *Experimental stress-strain relationship for cement concrete under biaxial compression*, in: Proceedings of the International Conference on Concrete and Concrete Structures, 28-29 April 1999, Žilina, 47-54.
23. Litewka A.: *Effective material constants for orthotropically damaged elastic solid*, Archives of Mechanics, **37**, 6 (1985) 631-642.
24. Litewka A., Bogucka J., Dębiński J.: *Deformation induced anisotropy of concrete*, Archives of Civil Engineering, **42**, 4 (1996) 425-445.
25. Litewka A., Bogucka J., Dębiński J.: *Anisotropic behaviour of damaged concrete and fibre reinforced concrete*, in: Anisotropic Behaviour of Damaged Materials, eds., J. Skrzypek, A. Ganczarski, Berlin-Heidelberg, Springer Verlag 2003, 185-219.
26. Litewka A., Dębiński J.: *Damage-induced anisotropy and deformability of brittle rock-like materials*, Key Engineering Materials, **230-232**, (2002) 505-508.
27. Litewka A., Dębiński J.: *Load-induced oriented damage and anisotropy of rock-like materials*, Int. Journal of Plasticity, **19**, (2003) 2171-2191.

28. Litewka A., Lis Z.: *Creep rupture of metals under tri-axial state of stress*, in: Creep in Structures, ed. M. Życzkowski, Berlin-Wien, Springer Verlag 1991, 371-378.
29. Majewski S.: *Mechanics of structural concrete in terms of elasto-plasticity*, Gliwice, Wydawnictwo Politechniki Śląskiej 2003, (in Polish).
30. Mitrofanov V.P., Dovzenko O.A.: *Development of deformation induced anisotropy of concrete under uni-axial compression*, Beton Zelezobeton, 10 (1991) 9-11, (in Russian).
31. Murakami S.: *Progress in continuum damage mechanics*, J.S.M.E. International Journal, **30**, (1987) 701-710.
32. Murakami S., Kamiya K.: *Constitutive and damage evolution equations of elastic-brittle materials based on irreversible thermodynamics*, International Journal of Mechanical Sciences, **39**, 4 (1997) 473-486.
33. Neville A.M.: *Properties of concrete*, Harlow, Longman 1995.
34. Rummel F.: *Brittle fracture of rocks*, in: Rock mechanics, Ed.: L. Muller, Wien, Springer-Verlag 1972, 85-94.
35. Szojda L.: *Possibilities of numerical analysis of masonry structure*, Proceedings of XLVII Scientific Conference, 16-21 September 2001, Opole-Krynica, Vol. 3, 385-392, (in Polish).
36. Szojda L.: *Analysis of interaction of masonry structures and deformable foundation*, PhD Thesis, Silesian University of Technology, Gliwice 2001, (in Polish).
37. Szojda L., Majewski S.: *Numerical simulation of complex stress-state in masonry structure,* Proceedings of the Sixth International Masonry Conference, London, 4-6 November 2002, 471-476.
38. Thienel K.-Ch., Rostasy F.S., Becker G.: *Strength and deformation of sealed HTR-concrete under bi-axial stress at elevated temperature*, in: Transactions of 11th Int. Conference on Structural Mechanics in Reactor Technology, Vol. H, Atomic Energy Society of Japan, Tokyo 1991, 73-78.
39. Yazdani S., Karnawat S.: *A constitutive theory for brittle solids with application to concrete,* Int. Journal of Damage Mechanics, **5,** 1 (1996) 93-110.

BADANIE MATERIAŁÓW KRUCHYCH W STANIE TRÓJOSIOWYM: MOTYWACJA, TECHNIKA BADAŃ, WYNIKI

S t r e s z c z e n i e

Postęp w mechanice materiałów wymaga szerokich, wzajemnie ze sobą powiązanych teoretycznych i doświadczalnych badań właściwości mechanicznych materiałów konstrukcyjnych. Jest to konieczne szczególnie wtedy gdy stosowane są materiały nowe a także wtedy, gdy istnieje potrzeba opracowania zaawansowanego modelu teoretycznego niezbędnego do opisu procesów fizycznych zachodzących w materiale poddanym złożonemu stanowi naprężenia. Celem tej pracy jest uzyskanie nowych, ogólniejszych danych doświadczalnych dla kruchych materiałów badanych w trójosiowym stanie naprężenia oraz przedstawienie zastosowanej techniki badawczej. W tym celu cylindryczne próbki cegły i zaprawy przebadane zostały przy zastosowaniu dwóch różnych schematów obciążenia trójosiowego a także przy jednoosiowym ściskaniu niezbędnym dla uzyskania danych wstępnych służących do cechowania badanych materiałów. Drugim celem pracy jest zaprezentowanie możliwości zastosowania własnego modelu fenomenologicznego bazującego na mechanice uszkodzenia materiałów oraz na teorii reprezentacji funkcji tensorowych. Porównanie wyników teoretycznych otrzymanych przy użyciu tego modelu z rezultatami badań wykazało zadowalającą ich zgodność.